



| | |
|------------------|---|
| Title | Low-threshold and quasi-single-mode random laser within a submicrometer-sized ZnO spherical particle film |
| Author(s) | Fujiwara, Hideki; Niyuki, Ryo; Ishikawa, Yoshie; Koshizaki, Naoto; Tsuji, Takeshi; Sasaki, Keiji |
| Citation | Applied Physics Letters, 102(6), 061110 https://doi.org/10.1063/1.4792349 |
| Issue Date | 2013-02-11 |
| Doc URL | http://hdl.handle.net/2115/52231 |
| Rights | Copyright 2013 American Institute of Physics. This article may be downloaded for personal use only. Any other use requires prior permission of the author and the American Institute of Physics. The following article appeared in Appl. Phys. Lett. 102, 061110 (2013) and may be found at https://dx.doi.org/10.1063/1.4792349 |
| Type | article |
| File Information | APL102-6_061110.pdf |



[Instructions for use](#)

Low-threshold and quasi-single-mode random laser within a submicrometer-sized ZnO spherical particle film

Hideki Fujiwara, Ryo Niyuki, Yoshie Ishikawa, Naoto Koshizaki, Takeshi Tsuji et al.

Citation: *Appl. Phys. Lett.* **102**, 061110 (2013); doi: 10.1063/1.4792349

View online: <http://dx.doi.org/10.1063/1.4792349>

View Table of Contents: <http://apl.aip.org/resource/1/APPLAB/v102/i6>

Published by the [American Institute of Physics](#).

Related Articles

Numerical simulation of stimulated emission and lasing in dye doped cholesteric liquid crystal films
J. Appl. Phys. **113**, 063106 (2013)

Influence of the excitation area on the thresholds of organic second-order distributed feedback lasers
APL: Org. Electron. Photonics **5**, 256 (2012)

Influence of the excitation area on the thresholds of organic second-order distributed feedback lasers
Appl. Phys. Lett. **101**, 223303 (2012)

Gain- and feedback-channel matching in lasers based on radiative-waveguide gratings
Appl. Phys. Lett. **101**, 143507 (2012)

Single-mode lasing of GaN nanowire-pairs
Appl. Phys. Lett. **101**, 113106 (2012)

Additional information on *Appl. Phys. Lett.*

Journal Homepage: <http://apl.aip.org/>

Journal Information: http://apl.aip.org/about/about_the_journal

Top downloads: http://apl.aip.org/features/most_downloaded

Information for Authors: <http://apl.aip.org/authors>

ADVERTISEMENT

JANIS Does your research require low temperatures? Contact Janis today.
Our engineers will assist you in choosing the best system for your application.



10 mK to 800 K
Cryocoolers
Dilution Refrigerator Systems
Micro-manipulated Probe Stations

LHe/LN₂ Cryostats
Magnet Systems

sales@janis.com www.janis.com
Click to view our product web page.

Low-threshold and quasi-single-mode random laser within a submicrometer-sized ZnO spherical particle film

Hideki Fujiwara,^{1,a)} Ryo Niyuki,¹ Yoshie Ishikawa,² Naoto Koshizaki,³ Takeshi Tsuji,⁴ and Keiji Sasaki¹

¹Research Institute for Electronic Science, Hokkaido University, Sapporo, Hokkaido 001-0020, Japan

²Graduate School of Engineering, Kagawa University, Takamatsu, Kagawa 761-0396, Japan

³National Institute of Advanced Industrial Science and Technology, Tsukuba, Ibaraki 305-8565, Japan

⁴Institute for Materials Chemistry and Engineering, Kyushu University, Kasuga, Fukuoka 816-8580, Japan

(Received 24 January 2013; accepted 1 February 2013; published online 13 February 2013)

An unique random laser exhibiting quasi-single-mode and low lasing threshold is developed by a homogenized submicrometer-sized zinc oxide particle film dispersed with intentionally introduced polymer particles as point defects. Such unique random lasing is dominantly initiated at the defect sites, although multi-mode peaks with a collapsed broad emission spectrum are observed at the defect-free sites as in the conventional random lasers. Thus our proposed simple structure can possibly provide the controllability of lasing properties even in random structures. © 2013 American Institute of Physics. [<http://dx.doi.org/10.1063/1.4792349>]

Random lasers, which typically composed of randomly distributed scatterers and gain materials, have attracted much attention over the past decade because of their unique laser oscillation phenomena without a clear cavity structure.^{1–11} The random structures can be expected to be utilized for easily fabricated and low-cost applications such as surface-emitting devices, because the disorder (*i.e.*, simple nanoparticle assembly or self-generated surface roughness) plays an important role for randomly distributed feedback due to the interference effects of recurrent multiple scattered light. However, considering the potential applications, the randomness should also raise issues of lasing mode controllability such as wavelength, location, and number of lasing modes.

Several approaches had been proposed for the control of random lasing properties such as temperature control,¹² reducing structure size,^{13–15} limiting excitation area,^{16,17} volume fraction control,¹⁸ and use of resonant scatterers.^{19,20} We have also numerically proposed a method using size-monodispersed scatterers and an intentionally introduced defect sites where no scatterer was set.^{21–23} In this structure, both the controls of the resonant frequency and localization position would be, respectively, realized by introducing defect sites and adjusting the Mie resonances of individual scatterers. From our numerical results, by optimizing the structural parameters (*e.g.*, sizes and refractive indexes of scatterers and defects), we confirmed that random lasing could be dominantly initiated at the defect sites even in the random structure, which would be worked as an active center for lasing. However, experimental verification has not yet been performed.

In this paper, towards the experimental realization of our proposed structure, we examined random lasing properties induced in a random structure composed by submicrometer-sized ZnO spherical particles mixed with polymer particles as defects. From the results, we found that while the lasing properties measured at defect-free sites exhibited the same behaviors as conventional random lasers

(discrete multiple sharp peaks superposed on the collapsed emission spectrum), those at defects were markedly modified, such as limiting the lasing position at the defect site, suppressing the number of lasing modes, and lowering thresholds. From these results, we believe that our proposed method can strongly modify the lasing properties in random structures, which is thoroughly different from the lasing properties of conventional random lasers.

In the experiments, submicrometer-sized ZnO spherical particles were used as scatterers and gain media. To experimentally realize the proposed structure, because scatterers optimally sized to match the resonant wavelengths with the emission spectrum of ZnO particles must be used in the lasing experiments,^{21–24} we roughly estimated the optimal size of ZnO particles to be about 200 nm from Mie scattering theory; hence, the lasing would be expected to occur at the emission wavelength of ZnO around 380 nm. For this purpose, quasi-monodispersed ZnO particles with the diameter of about 200 nm were fabricated from commercially available ZnO particles (mean diameter 100 nm, Hakusitech) by using a laser-induced melting method. The experimental setup was essentially the same as that reported elsewhere.^{25,26} Briefly, ZnO particles dispersed in water were irradiated by nonfocused laser light of a Nd:YAG laser (wavelength 355 nm, duration time 6 ns, repetition rate 10 Hz), and the concentration, laser intensity, and exposure time were set at 0.2 mg/ml, 100 mJ/cm², and 90 min, respectively. Figures 1(a) and 1(b) show scanning electron microscope (SEM) images of ZnO particles before and after the laser-induced melting. We clearly found that melting caused the shapes of ZnO particles to be spherical having diameter of about 200 nm (mean diameter 212 nm) and the shape and size of ZnO particles were homogenized rather than those before laser induced melting. Then, we intentionally added a small amount of green fluorescent polystyrene particles (diameter 900 nm, Corefront) into the solution as point defects. By using fluorescent polymer particles, we can determine the positions of point defects by observing the green fluorescence image. After mixing fluorescent polymer

^{a)}Electronic mail: fuji@es.hokudai.ac.jp.

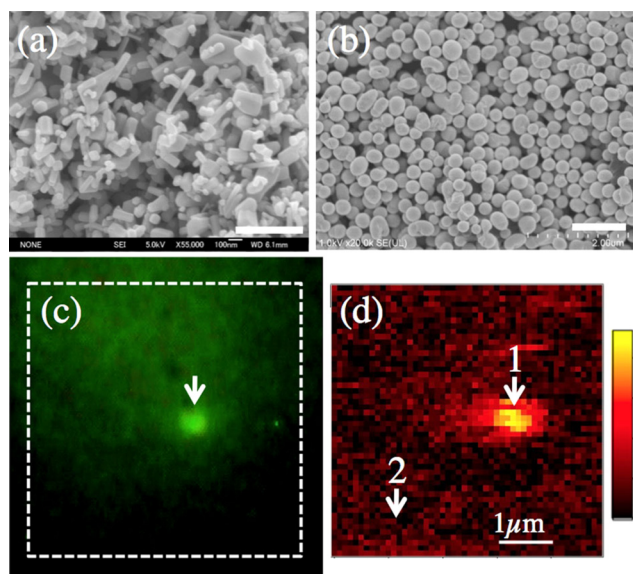


FIG. 1. Scanning electron micrograph of submicrometer-sized ZnO particles (a) before and (b) after laser-induced melting. White bars indicate the sizes of 500 nm in (a) and 1 μm in (b). (c) Fluorescence image of a polymer particle (arrow) and (d) emission intensity distribution of a ZnO particle film including a point defect. Dotted line in (c) suggests the scanned area of the intensity distribution. White arrows 1 and 2 in (d) represent the sites of spectral measurements, and arrow 1 also indicates the position of the polymer particle in (c).

particles, a drop of the solution was cast on a cover glass and dried (film thickness $\sim 100 \mu\text{m}$).

The sample was fixed on a piezo-stage set on a confocal microscope (Eclipse Ti-U, Nikon). Pulses from a Q-switched pulsed laser (wavelength 355 nm, duration time 100 ps, repetition rate 1 kHz) were irradiated on the sample by an objective lens ($100\times$, $\text{NA} = 0.9$, spot size $\sim 65 \mu\text{m}$). Emission from a ZnO particle film was collected by the same objective and passed through a pinhole (about 1 μm on the sample plane). Then, emission was coupled into a fiber bundle connected to a spectroscopy equipped with a cooled CCD camera and a photomultiplier tube (PMT). For lasing intensity distributions, signals from the PMT that detected photons with wavelengths from 375 to 395 nm passing through the spectrometer were recorded by two-dimensionally scanning the piezo-stage. After obtaining the intensity distribution, we measured the emission spectra at arbitrary sample positions and varying excitation intensity.

Figures 1(c) and 1(d) show the green fluorescence image (white arrow indicates the position of a polymer particle) and lasing intensity distribution of a ZnO particle film including a point defect (scanned area is indicated by a broken white line in Fig. 1(c)). From the results, an intense bright spot was observed in the intensity distribution and the spot position was almost the same as that of a fluorescent particle in Fig. 1(c), when the excitation intensity was maintained constant (10 MW/cm^2) during the scanning. Therefore, we confirmed that the emission intensity from ZnO particles was enhanced around the point defect rather than at the defect-free sites. Note that because fluorescent particles emitted only weak green light and were easily degraded by the irradiation of the excitation laser light, the emission from polymer particles did not contribute to obtained lasing experimental data.

Figure 2 shows the emission spectra measured at the point defect and defect-free site (indicated by white arrows 1 and 2 in Fig. 1(d)). Each figure shows the spectra with excitation intensities of 0.5, 1.0, and 2.0 times each threshold. In addition, the insets in each figure indicate the logarithmic plots of the peak intensities against the excitation intensities. In the figure, I_{d-th} and I_{th} indicate the thresholds at the point defect and defect-free site, which were defined as the first sharp peaks observed on a broad emission spectrum. From the excitation intensity dependences, because nonlinear evolutions of emission intensities were observed when the excitation intensity exceeded each threshold, we confirmed that random lasing was induced at the both of point defect and defect-free site. However, the threshold at the point defect (I_{d-th}) was about 6 MW/cm^2 , while that at the defect-free site (I_{th}) was 80 MW/cm^2 , which is about 13 times larger than that at the defect. Thus, at the excitation intensity of 10 MW/cm^2 ($\sim 1.5 \times I_{d-th}$ or $\sim 0.13 \times I_{th}$), the intense lasing spot was only observed at the defect, as shown in Fig. 1(d).

From the spectra at the defect-free site (arrow 2 in Fig. 1(d)), multi-mode sharp peaks superimposed on the collapsed broad emission spectrum were randomly appeared at the wavelengths around its gain maximum ($\sim 388 \text{ nm}$). In addition, relative peak intensities changed depending on the excitation intensities and each shot of the excitation pulses. These behaviors were also observed at different defect-free sites and were similar to the characteristics of conventional random lasers. Note that because the excitation intensity of $0.5 \times I_{th}$ was enough higher than the threshold at the defect (about $6 \times I_{d-th}$), broad emission spectrum already red-shifted compared with that at the defect owing to the increase in the exciton density or formation of electron-hole plasma with high excitation intensity.²⁷ On the other hand, when we measured at the point defect (arrow 1 in Fig. 1(d)), we found that the behaviors were clearly different from the results at the defect-free sites (conventional random lasers), where a single sharp peak was observed at 381 nm (see Fig. 2(b)). Increasing the excitation intensity up to five times of the threshold, the wavelength of the single discrete sharp peak did not fluctuate and no additional lasing peaks due to the increase in gain appeared. In addition, we could not clearly observe the collapse and red-shift of the broad

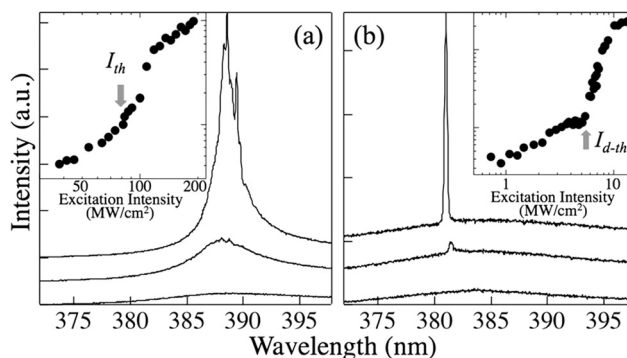


FIG. 2. Emission spectra measured at (a) defect-free and (b) defect sites (arrows 2 and 1 in Fig. 1(d)). The excitation intensities were 0.5, 1.0, and 2.0 times of each threshold from bottom to top. The insets in each figure show the excitation intensity dependences of peak intensities. Arrows indicate the threshold intensities (I_{th} and I_{d-th}), respectively.

emission spectra, as seen in Fig. 2(a), even when the excitation intensity exceeded the threshold; this resulted in a high contrast between a sharp discrete peak and the broad fluorescence spectrum.

To clarify the importance of the point defect, we also measured lasing spectra at different defect sites. Figures 3(a)–3(c) show lasing spectra measured at different defects. We clearly found that the obtained results were similar to those in Fig. 2; relatively intense spots at the defect, a few discrete sharp peaks, and lower thresholds were observed. By repeating similar measurements at different point defects, we found that single-peak lasing was observed at a rate of about 30% and a few lasing peaks appeared in about 70% of defects. Note that if polymer particles were placed on or near the surface of ZnO particle film, it was impossible to observe lasing behavior owing to huge leakage loss, and these cases were excluded. We summarized their lasing properties in Fig. 3(d), which indicates the scatter plots of the wavelength of the first lasing peaks and its thresholds at point defects and defect-free sites (indicated by squares and circles, respectively). From the results, we clearly confirmed that the intense lasing spots were observed at the defects and their lasing peaks at the defect sites always appeared at the wavelengths around 380 nm with the lasing thresholds of about 10 times lower than those at defect-free sites. Note that the lasing wavelengths at the defect-free sites seem to be more concentrated around 388 nm than those at point defects around 380 nm, because several lasing peaks simultaneously appeared at the defect-free sites and we plotted the center wavelengths of these multi-mode lasing.

Furthermore, also to clarify the importance of the homogenization of ZnO particles, we also measured the random structure composed of point defects and ZnO particles before the laser-induced melting. Figures 4(a) and 4(b) show the emission spectra and the intensity distribution including a defect (indicated by a black arrow), and the inset in Fig. 4(a) indicates the excitation dependence of lasing peak

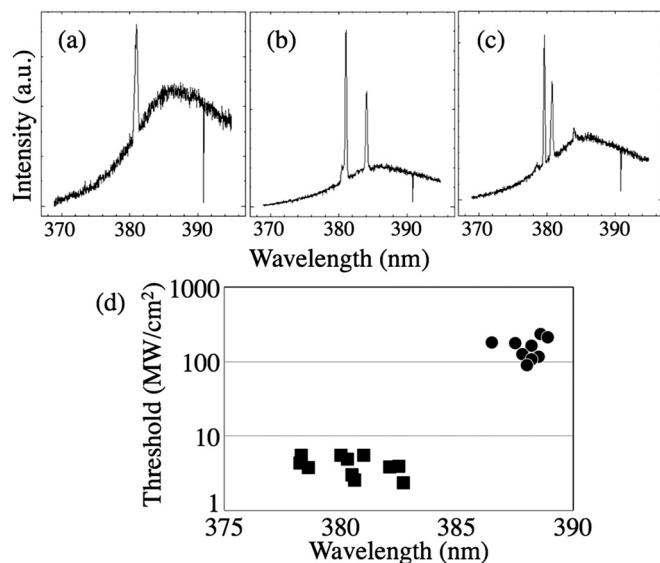


FIG. 3. (a)–(c) Emission spectra measured at different defects and (b) scatter plots of thresholds and lasing wavelengths. Solid squares and circles indicate the results at defects and defect-free sites. Vertical axis is logarithmically plotted.

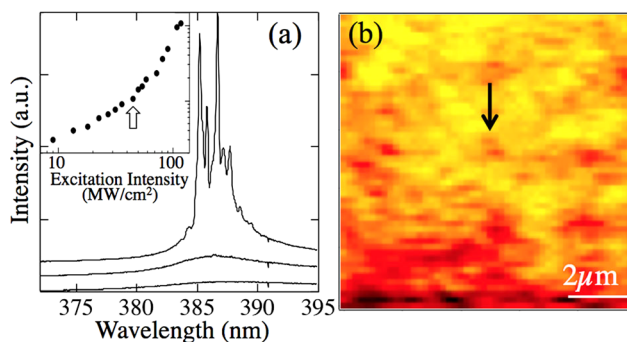


FIG. 4. (a) Emission spectra and (b) intensity distribution of a random structure composed of a point defects and ZnO particles before laser-induced melting. In (a), the excitation intensities were 0.5, 1.0, and 2.0 times of the threshold from bottom to top. In (b), the excitation intensity was kept constant at twice of the threshold.

intensity. The spectra in Fig. 4(a) were measured with the excitation intensities of 0.5, 1.0, and 2.0 times of the threshold. From the spectra measured at the defect, multiple sharp peaks superposed on a collapsed broad emission spectrum were observed at the wavelengths around 387 nm with the threshold of about 50 MW/cm², similar to the characteristics of conventional random lasers. Furthermore, from Fig. 4(b), we found that the intensity distribution shows almost uniform distribution (excitation intensity was kept at the twice of the threshold), although the defect particle existed at the center of the structure (indicated by a black arrow). These similar behaviors were repeatedly observed at different places and samples, and were thoroughly different from the results of random lasers composed of homogenized ZnO particles and point defects. Thus, from these results, although we must note that scatterers still have slight polydispersity (about 10%) even after the laser-induced melting, which may degrade the averaged resonant properties of a ZnO particle film, we concluded that not only the introduction of point defects but also the homogenization of ZnO particles would attribute to the modification of random lasing properties such as lasing wavelength, number of lasing modes, lasing sites, and thresholds.

In summary, we experimentally demonstrated random lasing from a random structure composed of homogenized ZnO particles including polymer particles as point defects. Comparing the random lasing properties at point defects and defect-free sites, we confirmed that the lasing behaviors were markedly modified at the defect. In addition, the random lasing properties at a defect within a random structure composed of ZnO particles before the laser-induced melting were almost same as those at defect-free sites and conventional random lasers. Thus, by simply introducing polymer particles into homogenized ZnO particles, we demonstrated unique random lasing properties such as limiting the lasing position at the defect site, suppressing the number of lasing modes, and lowering the thresholds. Even though further investigation is necessary to understand these observed unique random lasing properties, we believe that our results will provide important viewpoints for manipulating randomly appearing resonant and lasing properties in random structures.

This work was supported by the PRESTO program of the Japan Science and Technology Agency, Grant-in-Aids

for Young Scientists (A) (22681011), Exploratory Research (24651111), and Scientific Research (C) (21020027) from the Ministry of Education, Culture, Sports, Science and Technology of Japan, and the Cooperative Research Program of the Network Joint Research Center for Materials and Devices (Institute for Materials Chemistry and Engineering, Kyushu University).

- ¹M. A. Noginov, *Solid-State Random Lasers* (Springer, New York, 2005).
- ²D. S. Wiersma, *Nat. Phys.* **4**, 359 (2008).
- ³K. L. van der Molen, R. W. Tjerkstra, A. P. Mosk, and A. Lagendijk, *Phys. Rev. Lett.* **98**, 143901 (2007).
- ⁴K. Firdaus, T. Nakamura, and S. Adachi, *Appl. Phys. Lett.* **100**, 171101 (2012).
- ⁵S. Murai, K. Fujita, J. Konishi, K. Hirao, and K. Tanaka, *Appl. Phys. Lett.* **97**, 031118 (2010).
- ⁶M. Sakai, Y. Inose, K. Ema, T. Ohtsuki, H. Sekiguchi, A. Kikuchi, and K. Kishino, *Appl. Phys. Lett.* **97**, 151109 (2010).
- ⁷Q. Li, K. Gao, Z. Hu, W. Yu, N. Xu, J. Sun, and J. Wu, *J. Phys. Chem. C* **116**, 2330 (2012).
- ⁸C. T. Dominguez, R. L. Maltez, R. M. S. dos Reis, L. S. A. de Melo, C. B. de Araújo, and A. S. L. Gomes, *J. Opt. Soc. Am. B* **28**, 1118 (2011).
- ⁹R. G. S. El-Dardiry and A. Lagendijk, *Appl. Phys. Lett.* **98**, 161106 (2011).
- ¹⁰H. Fujiwara and K. Sasaki, *Jpn. J. Appl. Phys.* **43**, L1337 (2004).
- ¹¹H. Fujiwara and K. Sasaki, *Appl. Phys. Lett.* **89**, 071115 (2006).
- ¹²D. S. Wiersma and S. Cavalieri, *Nature* **414**, 708 (2001).
- ¹³H. Cao, J. Y. Xu, D. Z. Zhang, S.-H. Chang, S. T. Ho, E. W. Seeling, X. Liu, and R. P. H. Chang, *Phys. Rev. Lett.* **84**, 5584 (2000).
- ¹⁴H. Cao, J. Y. Xu, E. W. Seeling, and R. P. H. Chang, *Appl. Phys. Lett.* **76**, 2997 (2000).
- ¹⁵C. Vanneste and P. Sebbah, *Phys. Rev. E* **71**, 026612 (2005).
- ¹⁶G. V. Soest, M. Tomita, and A. Lagendijk, *Opt. Lett.* **24**, 306 (1999).
- ¹⁷P. Sebbah and C. Vanneste, *Phys. Rev. B* **66**, 144202 (2002).
- ¹⁸T. Nakamura, B. P. Tiwari, and S. Adachi, *Appl. Phys. Lett.* **99**, 231105 (2011).
- ¹⁹H. Noh, J.-K. Yang, S. F. Liew, M. J. Rooks, G. S. Solomon, and H. Cao, *Phys. Rev. Lett.* **106**, 183901 (2011).
- ²⁰S. Gottardo, R. Sapienza, P. D. Garcia, A. Blanco, D. S. Wiersma, and C. Lopez, *Nat. Photonics* **2**, 429 (2008).
- ²¹H. Fujiwara, Y. Hamabata, and K. Sasaki, *Opt. Express* **17**, 3970 (2009).
- ²²H. Fujiwara, Y. Hamabata, and K. Sasaki, *Opt. Express* **17**, 10522 (2009).
- ²³H. Fujiwara, T. Ikeda, and K. Sasaki, *Jpn. J. Appl. Phys.* **49**, 112002 (2010).
- ²⁴H. Miyazaki, M. Hase, H. T. Miyazaki, Y. Kurokawa, and N. Shinya, *Phys. Rev. B* **67**, 235109 (2003).
- ²⁵Y. Ishikawa, Q. Feng, and N. Koshizaki, *Appl. Phys. A* **99**, 797 (2010).
- ²⁶H. Q. Wang, N. Koshizaki, L. Li, L. C. Jia, K. Kawaguchi, X. Y. Li, A. Pyatenko, Z. Swiatkowska-Warkocka, Y. Bando, and D. Golberg, *Adv. Mater.* **23**, 1865 (2011).
- ²⁷G. Tobin, E. McGlynn, M. O. Henry, J.-P. Mosnier, E. de Posada, and J. G. Lunney, *Appl. Phys. Lett.* **88**, 071919 (2006).